

---

# ConBO: Conditional Bayesian Optimization

---

Michael Pearce<sup>1</sup> Janis Klaise<sup>2</sup> Matthew Groves<sup>3</sup>

## Abstract

Bayesian optimization is a class of data efficient model based algorithms typically focused on global optimization. We consider the more general case where a user is faced with multiple problems that each need to be optimized conditional on a state variable, for example we optimize the location of ambulances conditioned on patient distribution given a range of cities with different patient distributions. Similarity across objectives boosts optimization of each objective in two ways: in modelling by data sharing across objectives, and also in acquisition by quantifying how all objectives benefit from a single point on one objective. For this we propose ConBO, a novel efficient algorithm that is based on a new hybrid Knowledge Gradient method, that outperforms recently published works on synthetic and real world problems, and is easily parallelized to collecting a batch of points.

## 1. Introduction

Expensive black box functions arise in many fields such as fluid simulations (Picheny & Ginsbourger, 2013), engineering wing design (Jeong et al., 2005), and machine learning parameter tuning (Snoek et al., 2012). In this work we consider the more general case where the expensive function must be optimized for a range of settings, or conditioned on a *state*, often called a context or a nuisance variable. This has many applications as follows.

**Physics simulators:** Ginsbourger et al. (2014) learn the optimal packing fraction of particles in a container for each possible particle size. Char et al. (2019); Chung et al. (2020) learn the optimal controls of a nuclear fusion reactor for each plasma state.

**Algorithm Parameter Tuning:** Bardenet et al. (2013)

---

<sup>1</sup>Centre for Complexity Science, Warwick University, Coventry, United Kingdom <sup>2</sup>Seldon Technologies, London, United Kingdom <sup>3</sup>Centre for Doctoral Training in Mathematics for Real-World Systems, Warwick University, Coventry, United Kingdom. Correspondence to: Michael Pearce <scrambledpie@gmail.com>.

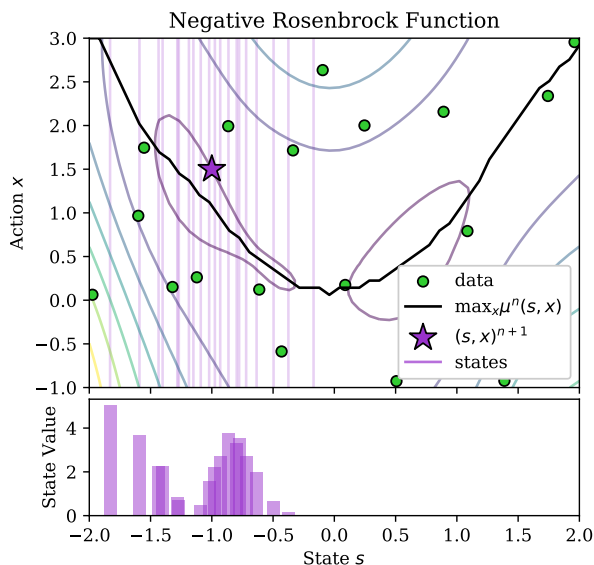


Figure 1. Top: GP model. Each state (vertical slice) is an objective function to maximise. A new sample  $(s, x)^{n+1}$  provides information about the optima of similar states. Bottom: the acquisition function value of each state using hybrid Knowledge Gradient.

learn optimal hyperparameters for each dataset in a collection of datasets. Smith-Miles et al. (2014) take a range of graphs and learn the best coloring algorithm for each graph.

**Robust Engineering:** when designing a wing for a range of operating temperatures, an engineer needs to know the *worst case* performance of the wing for each temperature.

**Logistics:** Given a range of warehouses that each face different sales demand, a user needs to optimize the stock controller of each warehouse (Poloczek et al., 2016). Given a range of cities with different population distributions, for each city a user must optimize the base location of a set of ambulances. In this work, we consider these two applications.

Since evaluating such a black box could entail minutes to days of computation, optimizing the black box requires a data efficient algorithm. For this, Bayesian optimization (BO) has become a very popular and powerful class of algorithms. BO typically uses Gaussian process regression (GP), or Kriging, to build a prediction model of the black box with uncertainty estimates. This is then combined with an

acquisition function that quantifies the benefit of evaluating a new output of the expensive function, popular choices of acquisition function include Expected Improvement (EI) (Jones et al., 1998), Entropy Search (Hennig & Schuler, 2012), Knowledge Gradient (Frazier et al., 2009), Upper Confidence Bound (Kandasamy et al., 2016) amongst many others. The input with largest benefit is chosen for evaluation, added to the model’s dataset and the algorithm repeats. For reviews, see Shahriari et al. (2015); Frazier (2018).

Many problem scenarios have been widely studied in the Bayesian optimization literature, small and large scale global optimization (Jones et al., 1998; Scott et al., 2011; Wang et al., 2013; Eriksson et al., 2019), multi-objective (Knowles, 2006; Belakaria et al., 2019), maximising an average over objectives (Swersky et al., 2013; Pearce & Branke, 2017; Toscano-Palmerin & Frazier, 2018), and maximising an expensive function with access to a cheaper approximation (Huang et al., 2006; Poloczek et al., 2017; Kandasamy et al., 2017).

For the rest of this work we shall refer to variables that are to be optimized as *actions*, though parameters, decision variables, and solutions are often used. There are many variations of the conditional setting. Optimization with warm starts/dynamic environments/transfer learning Morales-Enciso & Branke (2015); Feurer et al. (2015); Poloczek et al. (2016); Perrone et al. (2018) may be interpreted as the problem of optimizing a moving objective, the time index is a state variable that intermittently changes outside of user control. This is applied to a variation of the many warehouses example mentioned above and to hyperparameters of neural networks. Krause & Ong (2011) propose a BO algorithm for the recurrent contextual setting. At each iteration the context (or state) is passed to the user who then chooses an action. The considered applications include drug design in which the algorithm visits molecules (states) in a round-robin fashion and chooses a test chemical (action) at each iteration. Many applications in these works may also be viewed as serialised versions of conditional optimization problems. In drug design, an experimenter may be free to choose the molecule for each test; in hyperparameter tuning, if a collection of datasets is already in user possession, they can freely choose the dataset and parameters to train next. Mathematically, the state is within user control, and the user aims to *maximise all objectives simultaneously*. Others have referred to this as finding profile optima or conditional optima, for simplicity here we refer to this general problem as *conditional* optimization (admittedly at the risk of overloading the term) in order to avoid any confusion with recurrence or time dependence implied by other names.

Previous conditional Bayesian optimization algorithms include the SCoT algorithm of Bardenet et al. (2013) that visits states in a round-robin fashion and chooses actions using

expected improvement. The Profile Expected Improvement (PEI) algorithm of Ginsbourger et al. (2014) considers continuous state and proposes an acquisition function that measures expected improvement of a new outcome over the best predicted outcome within the same state. The PEQI method of Sambakhé et al. (2019) extends PEI to noisy problems. Pearce & Branke (2018) propose the REVI algorithm that quantifies the benefit a new sample will have on all states and is the starting point for the approach we develop here. Most recently, Char et al. (2019) propose a novel kernel with a length scale that varies across states and a multi-task Thompson sampling method (MTS) for collecting new data. While REVI and MTS appear to be the strongest algorithms in this setting, REVI has drawbacks. It suffers from expensive computation, requires a discretization over the state and action domains that cannot scale to more than a few dimensions, and was only tested on toy functions. As we will discuss later, there are fundamental aspects of conditional optimization that are not exploited by MTS and this algorithm can also be improved upon. We propose ConBO, a well principled, fast, more scalable algorithm that collects each data point to maximize all objectives, is optimized by gradient ascent, and outperforms PEQI, REVI and MTS in a variety of synthetic and real world applications.

## 2. Problem Statement

Adopting the terminology of bandits, we assume that we have an expensive black box function that takes as input both a *state* in state space  $s \in S$  and an *action* in action space  $x \in X$  either of which may be continuous or discrete. The expensive function returns a noisy scalar *reward*,

$$f(s, x) : S \times X \rightarrow \mathbb{R}. \quad (1)$$

There is a distribution over states  $\mathbb{P}[s]$  that encodes the priority or weighting of states. Given a budget of  $N$  function calls, we aim to sequentially choose points  $(s, x)$  and observe a noisy reward  $f(s, x)$ . The objective is to learn the best action for every state, or a policy  $\pi : S \rightarrow X$ , that maximises expected output for all states

$$\text{Total Reward} = \int_S \mathbb{E}[f(s, \pi(s))] \mathbb{P}[s] ds \quad (2)$$

where the expectation is over the stochasticity in rewards. If there is only a single state, the reward function is a single objective, the policy is a single action, and the problem reduces to global optimisation. We use the general notation of continuous  $s \in S$ , however  $S$  may be a finite set and the integral reduces to a summation.

In this work we consider two simulators from operations research; cast in this framework they are as follows.

**Ambulances in a square:** (Dong et al., 2017) the action space is the  $(x, y)$  locations of three ambulance bases across

a  $30km \times 30km$  city,  $x \in X = [0, 30]^6$ . There is a range of cities each with a different population distribution, the state defines the mode of population density,  $s \in S = [0, 30]^2$ . The state density is the frequency of cities whose population is densest at  $s$ .  $\mathbb{P}[s]$  is a truncated Gaussian around the centre of the map, most cities, like London UK, are densest in the centre while others are densest at a coast line such as Singapore or Hong Kong. For a given city  $s$ , the objective is to find locations  $a$  that minimise expected ambulance journey times from bases to patients averaged over a simulated day  $\mathbb{E}[f(s, x)]$ .

**Assemble to order:** (Xie et al., 2016) a warehouse must choose target stocking levels  $x \in X = [0, 20]^8$  below which more stock will be requested. Meanwhile, stock is depleted as customer orders arrive and are fulfilled. The optimal restocking level  $x$  depends on the customer demand faced by a given warehouse, a scalar parameter  $s \in [0.5, 1.5]$ . The uniform state density  $\mathbb{P}[s]$  is the distribution of demands faced by different warehouses. The stochastic output  $f(s, x)$  is the profit from fulfilled orders minus holding costs over a month.

### 3. The General ConBO Algorithm

We first discuss the fitting of the Gaussian process model and the policy. We then motivate the acquisition value for a single state and how this is integrated over states yielding the acquisition function. We propose Hybrid Knowledge Gradient as a solution to the computational burden of conditional optimization. We finally demonstrate how to easily construct a batch for parallel evaluation using sequential penalization.

At a stage after having observed  $n$  data points,  $\{(s^i, x^i, y^i)\}_{i=1}^n$  where  $y^i = f(s^i, x^i)$ , we fit a Gaussian process from the joint space  $S \times X$  to outputs  $y \in \mathbb{R}$ . Let  $\tilde{X}^n = ((s, x)^1, \dots, (s, x)^n)$  and  $Y^n = (y^1, \dots, y^n)$ . A Gaussian process is defined by a prior mean and prior covariance function, we assume constant prior mean  $\mu^0(s, x) = \mu$  and Matérn covariance function. For specific applications one may incorporate expert knowledge through constructing bespoke mean functions and kernels, for more information see Rasmussen & Williams (2004). After observing data, predictions are given by

$$\mu^n(s, x) = \quad (3)$$

$$\mu^0(s, x) + k^0(s, x, \tilde{X}^n)K^{-1}(Y^n - \mu^0(\tilde{X}^n))$$

$$k^n(s, x, s', x') = \quad (4)$$

$$k^0(s, x, s', x') + k^0(s, x, \tilde{X}^n)K^{-1}k^0(\tilde{X}^n, s', x')$$

where  $K = k^0(\tilde{X}^n, \tilde{X}^n)$ . At test time, when faced with a state  $s$ , the predicted optimal action  $x$  defines a policy from

states to actions

$$\pi^n(s) = \arg \max_x \mu^n(s, x). \quad (5)$$

Collecting one data point at  $(s, x)^{n+1}$  will help learn the peak of all states, thereby improving the policy. To construct an acquisition function for conditional optimization, we start by looking for standard acquisition functions that account for how the model changes at unsampled locations  $(s', x') \neq (s, x)^{n+1}$ . The popular Expected improvement (EI) and upper confidence bound (UCB) are both functions of the mean and variance at the sampled point only  $\mu^n((s, x)^{n+1})$ ,  $k^n((s, x)^{n+1}, (s, x)^{n+1})$  and are thus blind to changes at  $(s', x')$ . Suitable families of acquisition functions include Entropy search that measures the mutual information between the new output  $\mathbb{P}[y^{n+1}|x^{n+1}]$  and the (induced) location of the peak  $\mathbb{P}[x^*|\tilde{X}^n, Y^n]$ , Max value entropy search (Wang & Jegelka, 2017) measures mutual information between the new output  $\mathbb{P}[y^{n+1}|x^{n+1}]$  and the largest output  $\mathbb{P}[\max y|\tilde{X}^n, Y^n]$ , Knowledge Gradient measures the expected change in peak posterior mean  $\mathbb{E}[\max \mu^{n+1}(x)]$  caused by  $y^{n+1}$ . These ‘‘globally aware’’ acquisition functions are naturally more expensive to compute than EI or UCB and in many applications are more sample efficient. In the conditional optimization case, (as we show next) the acquisition function must be evaluated once for each state and integrated over states further multiplying the computational cost. The framework we follow allows for any method and here we follow previous work adopting the Knowledge Gradient (KG). However, to mitigate the expense of integrating over states, in Section 3.2, we propose a simple fast implementation of KG.

#### 3.1. From Global to Conditional

Each  $s_i$  value defines a single global optimization problem over  $x \in X$ . In the case of KG, the acquisition value for state  $s_i$  given the new sample at  $(s, x)^{n+1}$  is the expected peak posterior mean over actions  $x$  with state  $s_i$ , we denote this as  $\text{KG}_c(\cdot)$  given by

$$\text{KG}_c(s_i; (s, x)^{n+1}) = \quad (6)$$

$$\mathbb{E}_{y^{n+1}}[\max_{x'} \mu^{n+1}(s_i, x')|(s, x)^{n+1}] - \max_{x''} \mu^n(s_i, x''),$$

we return to this equation in Section 3.2. Similar expressions for Entropy Search and Max Value entropy search,  $\text{ES}_c(s_i, (s, x)^{n+1})$ , are just as easily derived and are given in the Supplementary Material. Integrating over states  $s_i$  yields the total acquisition value

$$\int_S \text{KG}_c(s; (s, x)^{n+1})\mathbb{P}[s]ds. \quad (7)$$

The integral over  $s$  cannot be computed analytically and so we use Monte-Carlo with importance sampling.

When using a kernel that factorises  $k(s, x, s', x') = \sigma_0^2 k_S(s, s') k_X(x, x')$ , like squared exponential or Matérn, similarity across states is encoded in  $k_S(s, s')$ . This naturally leads to the proposal distribution  $q(s|s^{n+1}) \propto k_S(s, s^{n+1})$ . In our experiments, we use the Matérn kernel and a Gaussian proposal distribution using  $s^{n+1}$  as mean and the state kernel length scales,  $l_s$ , as standard deviations

$$q(s|s^{n+1}) \sim \mathcal{N}(s|s^{n+1}, \text{diag}(l_s^2)). \quad (8)$$

In our experiments we generate  $n_s = 40$  samples  $S_{MC} = \{s_1, \dots, s_{n_s}\}$  and compute importance weights  $\mathbb{P}[s_i]/q(s_i|s^{n+1})$ . Finally the acquisition function is

$$\text{ConBO}(s, x) = \sum_{s_i \in S_{MC}} \frac{\mathbb{P}[s_i]}{q(s_i|s^{n+1})} \text{KG}_c(s_i; (s, x)).$$

The randomly sampled states  $S_{MC}$  are refreshed with each call to  $\text{ConBO}(s, x)$  and (for any KG implementation) the function is differentiable so that the optimal  $(s, x)^{n+1}$  may be found with a stochastic gradient ascent optimizer such as Adam (Kingma & Ba, 2014).

As  $\text{ConBO}(s, x)$  is simply a sum of acquisition functions, it inherits all the theoretical properties that are not violated by summation. For example, KG is a non negative quantity (see barcharts of Figure 2, provable via Jensen’s inequality) and KG reduces to zero as a single point is sampled infinitely often. Always collecting data at  $\arg \max KG(x)$  ensures the whole search space  $X$  is explored in the infinite budget limit. Thus  $\text{ConBO}(s, x)$  is non negative and zero at infinitely sampled points and therefore also explores all space  $S \times X$  in the infinite budget limit.

In practice, the function  $\text{KG}_c(s_i, (s, x)^{n+1})$  must be computed once for each sampled state  $s_i$ , the computational cost is  $n_s$  times the the global acquisition function equivalent. To alleviate this cost, we propose a novel efficient algorithm for computing KG.

### 3.2. Hybrid Knowledge Gradient

KG was originally proposed for BO by Frazier et al. (2009). Given a hypothetical new location  $x^{n+1}$ , the method quantifies the value of a new hypothetical observation  $y^{n+1}$  by the expected increase in the peak of the posterior mean

$$\text{KG}(x) = \mathbb{E}_{y^{n+1}} [\max_{x'} \mu^{n+1}(x') | x^{n+1} = x] - \max_{x''} \mu^n(x''). \quad (9)$$

However the peak of a Gaussian process mean has no direct formula and approximations are required. Previous works have computed  $\text{KG}(x)$  in one of two ways. For the first way, in Equation 9, note that the maximizations are over a continuous set  $x' \in X$  which may be replaced with a discrete set  $x' \in X_d \subset X$ . Note from Equation 3 that there is a *linear* relationship between any observed  $y^i$  and the

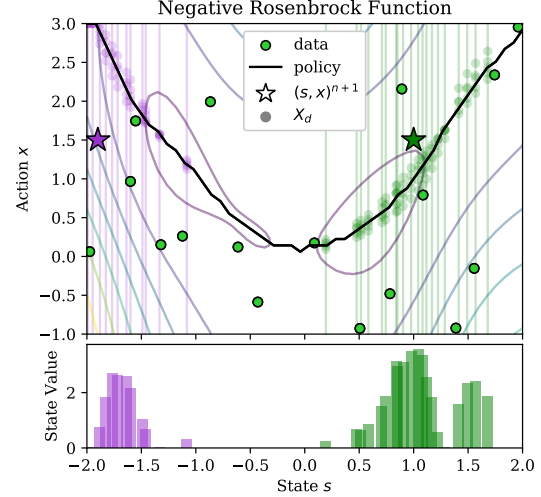


Figure 2. Top: the GP surface and two possible locations of  $(s, x)^{n+1}$ . The discretization computed by hybrid KG is shown for each state and is largely focused around the peak posterior mean. The left point is on a boundary and many influential stes are outside of state diminishing acquisition benefit. Bottom: hybrid KG for each state. The states affected by the two points do not overlap, if they are both peak of  $\text{ConBO}(s, x)$  then they may both be evaluated in parallel.

prediction at a point  $\mu^n(x_i)$  for all  $x_i \in X_d$ . Hence, each new prediction  $\mu^{n+1}(x_i)$  is a deterministic linear function of the random  $y^{n+1}$ . Thus  $\max \mu^{n+1}(X_d)$  is a deterministic *piece-wise linear* function of  $y^{n+1}$ . The expectation of the piece-wise linear function with Gaussian input  $y^{n+1}$  may be computed analytically and the output is a *lower bound* of the true  $\text{KG}(x)$  over the continuous set. We refer to this method as KG by discretization. This method suffers the curse of dimensionality, the number of points required to fill the space grows exponentially with dimension of  $X$  along with computational cost. Even when using a dense discretization,  $X_d$  may contain many unnecessary points  $x_i$  that do not form part of  $\max \mu^{n+1}(X_d)$ , see Figure 3 centre plot.

The second method for computing KG was designed to tackle these scaling problems. Given  $x^{n+1}$ , the method samples up to  $n_y = 1000$  values of  $y^{n+1}$  from the GP and for each value constructs  $\mu^{n+1}(x)$  (in  $O(n_y + n^2)$  time). Then the peak of each  $\mu^{n+1}(x)$  function is found using a continuous numerical optimizer such as L-BFGS. The resulting average of optimizer outputs is an *unbiased* estimate of  $\text{KG}(x)$  and we refer to this as KG by Monte-Carlo. However this can lead to much redundant computation as similar  $y^{n+1}$  values will have similar  $\max \mu^{n+1}(x)$  values, and the method does not explicitly make use of the linearity between  $y^{n+1}$  and  $\mu^{n+1}(x_i)$ , see Figure 3 centre right.

In this work, we instead propose a simple natural mixture of

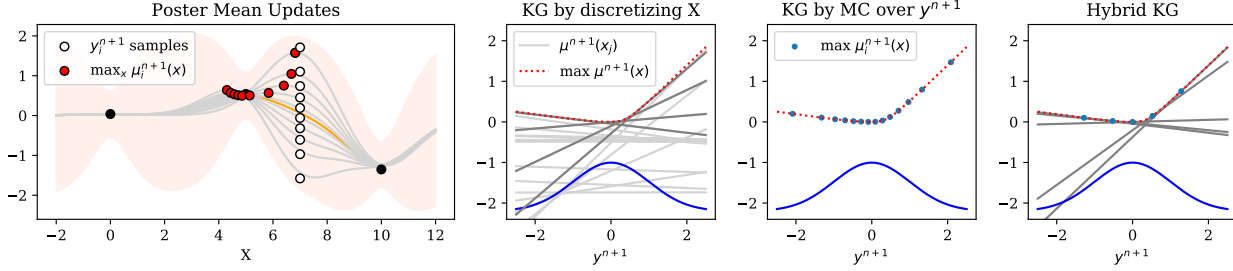


Figure 3. Methods for computing KG at  $x = 7$ . Left: realisations of  $\mu^{n+1}(x)$  with peaks. Middle left: discretizing the search space results in  $\max \mu^{n+1}(X_d)$  becoming a piece-wise linear function of  $y^{n+1}$  which may be integrated analytically. Dark lines show the relevant  $\mu^{n+1}(x_i)$ , the bell curve shows  $\mathbb{P}[y^{n+1}|x^{n+1}]$ . Middle-right: drawing up to 1000 samples of  $y^{n+1}$  and for each sample, invoking an optimizer to find  $\max \mu^{n+1}(x)$ . Right: our approach, using a fixed grid of  $n_y = 5$  values of  $y^{n+1}$ , optimize each  $\mu^{n+1}(x)$  and use each found  $x^*$  as a discretization point, all points are relevant.

the above two approaches we refer to as Hybrid KG. Given  $x^{n+1}$ , we use  $n_y \ll 1000$  values of  $y^{n+1}$ , construct each  $\mu^{n+1}(x)$  and find the peak using a numerical optimizer. We treat the set of discovered locations as an *optimized discretization*  $X_d = \{x_1^*, \dots, x_{n_y}^*\}$  to analytically compute  $\mathbb{E}[\max \mu^{n+1}(X_d)]$  lower bound of the true KG( $x$ ). This drastically reduces both redundant computation from unnecessary numerical optimizer calls and also removes all redundant points, all  $x_i \in X_d$  will contribute to  $\max \mu^{n+1}(X_d)$ . By increasing  $n_y$ , the lower bound can be arbitrarily tightened. In this work, we observed good performance with  $n_y = 5$ . The  $y^{n+1}$  values need not be stochastic, we use fixed spacing of the 0.1, 0.3, 0.5, 0.7, 0.9 quantiles of the  $\mathbb{P}[y^{n+1}|x^{n+1}]$  Gaussian distribution from the GP model. Figure 3 (right) shows how this is computed and Figure 2 shows the discretization for multiple states.

### 3.3. Batch Construction by Sequential Penalization

For global optimization, parallelizing BO algorithms to suggest a batch of  $q$  inputs,  $\{x^{n+1}, \dots, x^{n+q}\}$ , has been approached in multiple ways. For acquisition functions that compute an expectation over future outcomes  $\mathbb{P}[y^{n+1}|x^{n+1}]$ , (EI, KG, ES, MES), the acquisition value of a batch can be computed using the expectation over multiple correlated outcomes  $\mathbb{P}[y^{n+1}, \dots, y^{n+q}|x^{n+1}, \dots, x^{n+q}]$ . This larger  $q$  dimensional expectation, effectively looking  $q$  steps into the future, must be estimated by Monte-Carlo. At the same time, it is a function of all  $q$  points in the batch and must be optimized simultaneously over  $q$  times more dimensions  $X^q$ . This method of parallelization quickly becomes infeasible for even moderate dimensions and batch sizes. As before, adapting the method to conditional optimisation adds another layer of Monte-Carlo integration over  $s \in S$  multiplying the computational cost.

Thompson sampling (TS) randomly suggests the next point to evaluate,  $x^{n+1}$ . TS also has the convenient mathematical property that  $q$  step look ahead is equivalent to generating  $q$

i.i.d samples (Hernández-Lobato et al., 2017; Kandasamy et al., 2018). This property was used by Char et al. (2019) to parallelize MTS.

Alternatively, sequential construction of a batch can be done in  $O(q)$  time and we consider the method of González et al. (2016). First  $x^{n+1}$  is found by optimizing the chosen acquisition function  $x^{n+1} = \arg \max \alpha(x)$ . The acquisition function is then multiplied by a non-negative penalty function  $\phi(x, x^{n+1})$  that penalizes  $x$  similar to  $x^{n+1}$ . The next point is found by  $x^{n+2} = \arg \max_x \alpha(x)\phi(x^{n+1}, x)$ , then  $x^{n+3} = \arg \max_x \alpha(x)\phi(x^{n+1}, x)\phi(x^{n+2}, x)$  until a batch of  $q$  points is constructed. We use the inverted GP kernel as the penalty function

$$\phi((s, x), (s, x)^i) = 1 - \frac{k^0((s, x), (s, x)^i)}{k^0((s, x)^i, (s, x)^i)}.$$

See Figure 4 for an illustration. Previous work (Groves et al., 2018) showed that the conditional optimization setting is well suited to this construction method. Two points on dissimilar states do not interact and if they are both local peaks of the chosen acquisition function  $\alpha(s, x)$ , then both may both be evaluated in parallel, see Figure 2 for an example. In conditional optimization, the presence of state variables introduces multiple objective functions allowing a batch of points to be more spread out reducing interactions and possible inefficiencies. This can be achieved by penalization thus sidestepping the need for expensive nested Monte-Carlo integration. By contrast, in global optimization all  $q$  points are “crammed” into a single state, all interacting with the same objective requiring more care in batch construction techniques.

This method for batch construction may be applied to any acquisition function, in our experiments we apply it to REVI and ConBO.

In practice, we optimize the acquisition function using multi start gradient ascent and keep the entire history of evaluations  $\{(s_t, x_t, \alpha(s_t, x_t))\}_{t=1}^{\#calls}$ . Since this history is very

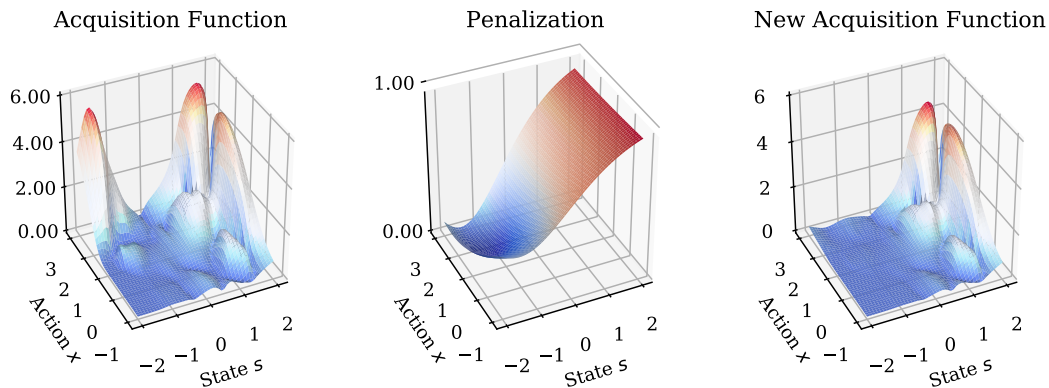


Figure 4. Left: acquisition function over  $S \times X$  with a peak at  $(s, x)^{n+1} = (-1.5, 2.5)$ , the first point in the batch. Centre: the penalization function that down-weights any point  $(s, x) \in S \times X$  according to similarity with  $(s, x)^{n+1}$ . Right: The product of acquisition and penalization functions, the peak at  $(s, x)^{n+2} = (1.6, 3.0)$  is the second point in the batch.

likely to contain multiple peaks, we simply apply the penalization to the set of past evaluations avoiding the need to re-optimize the penalized acquisition function. Therefore, efficiently parallelizing a conditional BO algorithm can be done in just a few additional lines of code.

#### 4. Risks in Conditional Optimization

The general conditional optimisation problem introduces subtle issues that do not emerge in global optimisation, here we briefly highlight them.

**Policy optimization vs data optimization:** Consider the case where the number of states,  $N_s$ , is significantly smaller than the sampling budget  $N_s \ll N$ . If many states are very similar, an algorithm learning the optimal action for each state,  $\arg \max_x \mathbb{E}[f(s, x)]$  or *policy optimization*, Specifically, an unsampled state,  $s_u$ , may be ignored if  $\arg \max_x \mathbb{E}[f(s_u, x)]$  is accurately known due to many similar surrounding sampled states  $s_s$ , there is little use in collecting data on  $s_u$ . However, for a user that wants to find good observations  $\max y$  for each state, or *data optimization*, such unsampled optimized-by-proxy states  $s_u$  will have very few observations and therefore rather poor  $\max y$ . Pearce & Branke (2018) suggested performing data efficient policy optimization first and reserving the final  $N_s$  for data optimization (therein called “risk averse”), allocating one sample per state with the action determined by EI. This yielded much better performance than performing (sub optimal) data optimization throughout. Alternatively, using MTS provides a compromise between policy and data optimization and showed mixed or better results than risk-averse REVI for data optimization. In general in the small state setting, these are competing goals and an algorithm must be designed with the goal in mind. In stochastic simulation optimization, a user is only interested in policy optimization; the best action will be deployed for long term use and

stochastic realizations of  $\max y$  observed during optimization are not the true long term reward  $\mathbb{E}[f(s, \pi(s))]$ . By contrast, global optimisation may be viewed as one state that receives *all* data points.

**Additive kernels:** (Kandasamy et al., 2015) Krause & Ong (2011) suggest using additive kernels for contextual optimization. Such kernels assume the function being modelled decomposes into a sum of functions, each one depending on an exclusive subset of variables. If the state variables and action variables are not in the same subsets then the assumed structure,  $f(s, x) = g(s) + h(x)$ , is reflected in the mean function  $\mu^n(s, x) = \mu_1^n(s) + \mu_2^n(x)$ . The policy becomes

$$\pi(s) = \arg \max_x \mu^n(s, x) = \arg \max_x \mu_1^n(x)$$

and the recommended action is *independent of state*, no method can learn the optimal action for each state and such partition should be avoided. If the inputs are partitioned such that either state variables or actions variable are in unique groups e.g.  $f(s_1) + g(s_2, x_2) + h(x_1)$ , then the non-interactive state variables  $s_1$  also do not affect the policy and therefore may be fixed to a constant, and the non-state dependent action variables  $x_1$  may be optimized while holding all other variables constant. In general, additive structure assumes *no interaction* between variables, conditional Bayesian optimization is only interesting *with interaction* between variables.

**State boundary effects:** when using a Gaussian process, collecting data at a given  $(s, x)^{n+1}$  point influences similar points  $(s', x')$  and the acquisition value of similar states may be computed using any globally aware acquisition function. When using a stationary kernel, if  $s^{n+1}$  is on the boundary of state space, much of the affected  $(s', x')$  points are outside of the set of feasible states and contribute no benefit thereby reducing total acquisition value. Sampling on state

boundaries provides less total information, see Figure 2. With higher state dimension, this effect becomes more and more significant as there are more state boundaries and high dimensional corners with exponentially fewer neighboring states. This effect is accounted for by acquisition functions that integrate over states like ConBO and REVI, but not for methods like PEI, PEQI or MTS.

## 5. Experiments

We perform numerical experiments on synthetic, low-dimensional functions and moderate-dimensional real world problems. We benchmark ConBO against the recently published conditional optimization algorithms PEQI, REVI and MTS. All algorithms use the same GP model, constant mean and Matérn kernel with hyperparameters learnt by maximum likelihood. For evaluation, we generate a set of test states and for each state, determine the action suggested by the learnt policy  $\arg \max_x \mu^n(s, x)$ . This state-action pair is repeatedly evaluated on the stochastic test problem to estimate true  $\mathbb{E}[f(s, \pi^n(s))]$ . The average of true qualities is reported. All experiments are averaged over 100 repetitions. We also performed experiments with alternative methods, K-nearest neighbor policy with epsilon greedy acquisition, uniform random search, normal global BO without conditioning on state, and found them all to be significantly worse and they may be found in the Supplementary Material.

### 5.1. Baselines

Implementation details are given in the Supplementary Material, here we provide quick summaries.

**PEQI:** given an  $(s, x)$  point, the expected improvement of the  $\beta$ -quantile of the GP,  $q_\beta(s, x)$  over the largest  $\beta$ -quantile with the same state  $\max_x q_\beta(s, x)$  capped by the largest output seen so far  $\min(\bar{y}, \max_x q_\beta(s, x))$  with  $\max y = \bar{y}$ .

**REVI:** at each iteration, sample states are drawn from  $\mathbb{P}[s]$  and actions are uniformly sampled from  $X$ . For each state, KG by discretization gives state value, the average over values yields REVI.

**MTS:** with a full discretization budget of 3000 points, a set of states is uniformly sampled from  $S$ , for each state  $s_i$  a bespoke discretization of  $X$  is made that includes  $\pi^n(s_i)$ , its neighbors, and random actions. A sample function  $\hat{f}$  is drawn from the GP. Using the sample as ground truth, the state is determined by comparing the highest reward for each state with the reward of the policy in each state then scaled by  $\mathbb{P}[s]$ ,  $s^{n+1} = \arg \max_{s_i} \left( \max_x \hat{f}(s_i, x) - \hat{f}(s_i, \pi(s_i)) \right) \mathbb{P}[s_i]$ . The corresponding most rewarding action of  $s^{n+1}$  is chosen.

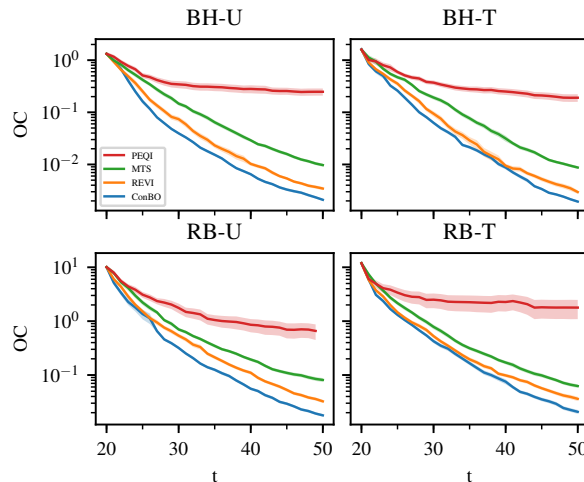


Figure 5. Test function opportunity cost. Top row: Branin-Hoo function with uniform (U) and triangular (T) state distributions. Bottom row: Rosenbrock function. The experiments were averaged over 100 trials and show the mean value and standard error.

### 5.2. Synthetic Functions

We use the standard Branin-Hoo and Rosenbrock functions that serve as a popular sanity check for BO algorithms. Since all methods use the same kernel and policy, these experiments demonstrate the benefits of the acquisition functions. We consider two state distributions, the uniform and triangular distribution peaked at the boundary of state space. This was used in (Pearce & Branke, 2018) as an adversarial case to differentiate methods, like PEQI and MTS, that only account for local state density but do not account for state boundary effects (Section 4).

Results are shown in Figure 5. In all cases we see that PEQI significantly falls behind the other methods and we drop PEQI from further experiments. Of the other methods, ConBO converges quickest towards the true optimal policy, followed by REVI and the MTS. In this low dimensional setting, the discretizations used in REVI are sufficient to fill the space and we see REVI and ConBO perform similarly. Contrary to prior work, there is very little difference between uniform and triangular results suggesting that MTS does not significantly suffer from the state boundary issue in these problems.

### 5.3. Warehouses and Ambulances

We also benchmark the algorithms on two larger problems commonly used in the simulation optimization literature, Ambulances in a Square (AMB) (Pasupathy & Henderson, 2011) and Assemble to Order (ATO) (Xie et al., 2016). For these, we further investigate the impact of parallel sample allocation on each algorithm.

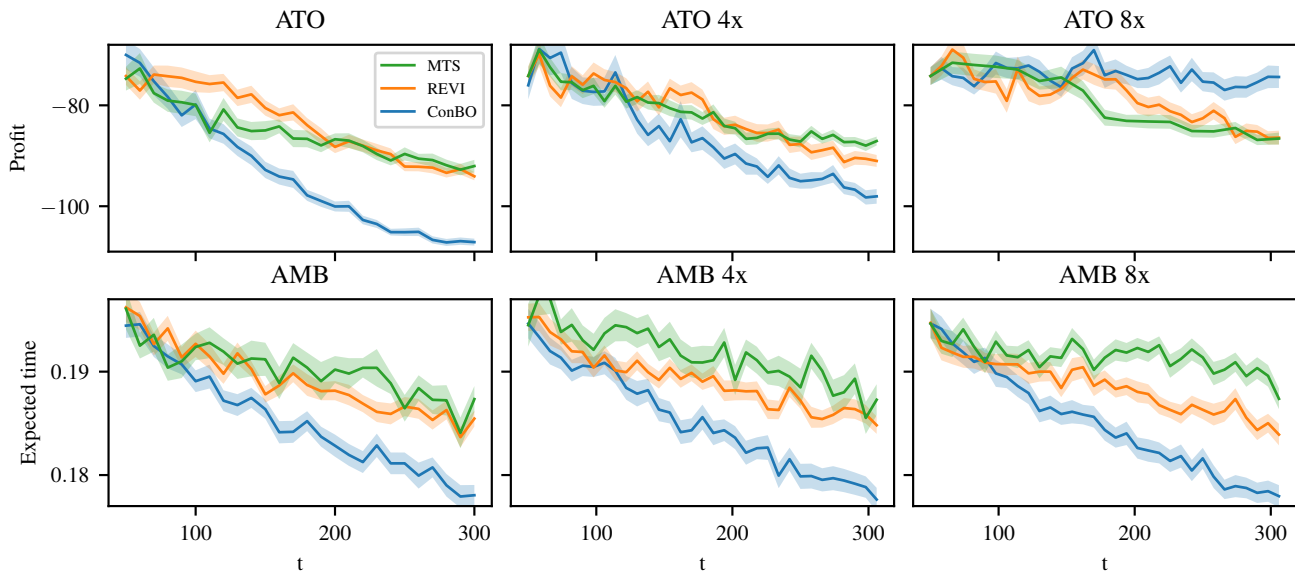


Figure 6. Algorithm performance on the Assemble To Order (top) and Ambulances (bottom) benchmarks. The left-most plots are with serial sample collection whilst 4x and 8x denote results with parallel sample collection with batch sizes of 4 and 8 points respectively. The experiments were averaged over 100 trials and show the mean value and standard error.

For both applications, we run each algorithm starting from 50 evaluations up to 300. The performance of each algorithm is measured on  $n_{test} = 250$  and  $n_{test} = 40$  test states for Ambulances and Assemble to order respectively. The test states are generated states from each  $\mathbb{P}[s]$  discussed in Section 2. Due to the cost of testing we only test every  $10^{th}$  iteration. Results are shown in Figure 6.

The Assemble to Order benchmark has a single state dimension and 8 action dimensions thus state boundary effects will be minimal while discretization over action space will require many points. In early testing, executing REVI with a large 9 dimensional discretization lead to memory errors and thus had to be reduced. ConBO with Hybrid KG using  $n_y = 5$  and  $n_s = 40$  has a total discretization of 200 points.

In serial mode,  $q = 1$ , ConBO provides the fastest convergence by a large margin. REVI and MTS are similar, both struggling with the higher dimension. As batch size increases, all algorithms deteriorate and in particular ConBO fails for large batch size. In further testing, this was reproduced when replacing the importance sampled states with a single set of random states frozen during each algorithm iteration (like REVI). This suggests that using hybrid KG (instead of KG by discretization as in REVI) causes the reduction in performance. We also observed that all algorithms significantly degrade when using the SE kernel while the relative ranking remains the same implying that the ATO benchmark in general is sensitive to algorithm design.

The Ambulance benchmark has two state dimensions and six actions dimensions hence boundary effects are more

important. In serial mode, ConBO again outperforms both recently published algorithms by a significant margin. Surprisingly, using standard EI for global optimization over all variables performed similarly to ConBO on this problem suggesting the algorithm has not converged at 300 points.

As batch size increases, there is almost no significant drop in performance for both ConBO and REVI implying the parallelism by penalization for conditional acquisition functions works very well.

## 6. Conclusion

We consider the problem of finding conditional optima and we refer to this as conditional Bayesian optimization. Bayesian optimization is especially useful in the small, expensive data regime. Algorithms need to be as data efficient as possible achieved by utilising the fundamental structure of a problem. In the case of conditional optimization, there are many structural features that can be baked into an algorithm. Firstly, one data point affects all optima and an efficient algorithm should exploit this fact, however, this necessitates a more sophisticated and expensive acquisition function. Secondly, batch evaluation of such expensive acquisition functions often leads to large Monte-Carlo integrals which, hypothetically, would also need to be modified to account for all states. We propose solutions to both of these challenges. We derive the general ConBO algorithm. This algorithm can be built on top of any globally aware acquisition function, inheriting theoretical results, and in this work we “slot in” Knowledge Gradient. It must be



computationally efficient and so we propose a novel hybrid KG. By observing that finding multiple optima can be done in parallel, the batch construction problem is also solved by simple penalization reducing large computations down to a few lines of code run in less than a second. Together this algorithm provides strong results, outperforming recently published baselines under ideal controlled settings and on non-trivial simulation optimization problems. In future work, we intend to apply the ConBO recipe to Max Value entropy Search, one of the quickest entropy based search algorithms.

## References

- Bardenet, R., Brendel, M., Kégl, B., and Sebag, M. Collaborative hyperparameter tuning. In *International Conference on Machine Learning*, pp. 199–207, 2013.
- Belakaria, S., Deshwal, A., and Doppa, J. R. Max-value entropy search for multi-objective bayesian optimization. In *Advances in Neural Information Processing Systems*, pp. 7823–7833, 2019.
- Char, I., Chung, Y., Neiswanger, W., Kandasamy, K., Nelson, A. O., Boyer, M., Kolemen, E., and Schneider, J. Offline contextual bayesian optimization. In *Advances in Neural Information Processing Systems*, pp. 4629–4640, 2019.
- Chung, Y., Char, I., Neiswanger, W., Kandasamy, K., Nelson, A. O., Boyer, M. D., Kolemen, E., and Schneider, J. Offline contextual bayesian optimization for nuclear fusion. *arXiv preprint arXiv:2001.01793*, 2020.
- Dong, N. A., Eckman, D. J., Zhao, X., Henderson, S. G., and Poloczek, M. Empirically comparing the finite-time performance of simulation-optimization algorithms. In *2017 Winter Simulation Conference (WSC)*, pp. 2206–2217. IEEE, 2017.
- Eriksson, D., Pearce, M., Gardner, J., Turner, R. D., and Poloczek, M. Scalable global optimization via local bayesian optimization. In *Advances in Neural Information Processing Systems*, pp. 5497–5508, 2019.
- Feurer, M., Springenberg, J. T., and Hutter, F. Initializing bayesian hyperparameter optimization via meta-learning. In *Twenty-Ninth AAAI Conference on Artificial Intelligence*, 2015.
- Frazier, P., Powell, W., and Dayanik, S. The knowledge-gradient policy for correlated normal beliefs. *INFORMS Journal on Computing*, 21(4):599–613, 2009. ISSN 10919856.
- Frazier, P. I. A tutorial on bayesian optimization. *arXiv preprint arXiv:1807.02811*, 2018.
- Ginsbourger, D., Baccou, J., Chevalier, C., Perales, F., Garland, N., and Monerie, Y. Bayesian adaptive reconstruction of profile optima and optimizers. *SIAM/ASA Journal on Uncertainty Quantification*, 2(1):490–510, 2014.
- González, J., Dai, Z., Hennig, P., and Lawrence, N. Batch bayesian optimization via local penalization. In *Artificial intelligence and statistics*, pp. 648–657, 2016.
- Groves, M., Pearce, M., and Branke, J. On parallelizing multi-task bayesian optimization. In *2018 Winter Simulation Conference (WSC)*, pp. 1993–2002. IEEE, 2018.
- Hennig, P. and Schuler, C. J. Entropy search for information-efficient global optimization. *Journal of Machine Learning Research*, 13(Jun):1809–1837, 2012.
- Hernández-Lobato, J. M., Requeima, J., Pyzer-Knapp, E. O., and Aspuru-Guzik, A. Parallel and distributed thompson sampling for large-scale accelerated exploration of chemical space. In *Proceedings of the 34th International Conference on Machine Learning-Volume 70*, pp. 1470–1479. JMLR. org, 2017.
- Huang, D., Allen, T. T., Notz, W. I., and Miller, R. A. Sequential kriging optimization using multiple-fidelity evaluations. *Structural and Multidisciplinary Optimization*, 32(5):369–382, 2006.
- Jeong, S., Murayama, M., and Yamamoto, K. Efficient optimization design method using kriging model. *Journal of aircraft*, 42(2):413–420, 2005.
- Jones, D. R., Schonlau, M., and Welch, W. J. Efficient global optimization of expensive black-box functions. *Journal of Global optimization*, 13(4):455–492, 1998.
- Kandasamy, K., Schneider, J., and Póczos, B. High dimensional bayesian optimisation and bandits via additive models. In *International Conference on Machine Learning*, pp. 295–304, 2015.
- Kandasamy, K., Dasarathy, G., Oliva, J. B., Schneider, J., and Póczos, B. Gaussian process bandit optimisation with multi-fidelity evaluations. In *Advances in Neural Information Processing Systems*, pp. 992–1000, 2016.
- Kandasamy, K., Dasarathy, G., Schneider, J., and Póczos, B. Multi-fidelity bayesian optimisation with continuous approximations. In *Proceedings of the 34th International Conference on Machine Learning-Volume 70*, pp. 1799–1808. JMLR. org, 2017.
- Kandasamy, K., Krishnamurthy, A., Schneider, J., and Póczos, B. Parallelised bayesian optimisation via thompson sampling. In *International Conference on Artificial Intelligence and Statistics*, pp. 133–142, 2018.

- Kingma, D. P. and Ba, J. Adam: A method for stochastic optimization. *arXiv preprint arXiv:1412.6980*, 2014.
- Knowles, J. Parego: a hybrid algorithm with on-line landscape approximation for expensive multiobjective optimization problems. *IEEE Transactions on Evolutionary Computation*, 10(1):50–66, 2006.
- Krause, A. and Ong, C. S. Contextual gaussian process bandit optimization. In *Advances in neural information processing systems*, pp. 2447–2455, 2011.
- Morales-Enciso, S. and Branke, J. Tracking global optima in dynamic environments with efficient global optimization. *European Journal of Operational Research*, 242:744–755, 2015.
- Pasupathy, R. and Henderson, S. G. Simopt: A library of simulation optimization problems. In *Proceedings of the 2011 Winter Simulation Conference (WSC)*, pp. 4075–4085, Dec 2011. doi: 10.1109/WSC.2011.6148097.
- Pearce, M. and Branke, J. Bayesian simulation optimization with input uncertainty. In *2017 Winter Simulation Conference (WSC)*, pp. 2268–2278. IEEE, 2017.
- Pearce, M. and Branke, J. Continuous multi-task bayesian optimisation with correlation. *European Journal of Operational Research*, 270(3):1074–1085, 2018.
- Perrone, V., Jenatton, R., Seeger, M. W., and Archambeau, C. Scalable hyperparameter transfer learning. In *Advances in Neural Information Processing Systems*, pp. 6845–6855, 2018.
- Picheny, V. and Ginsbourger, D. A nonstationary space-time gaussian process model for partially converged simulations. *SIAM/ASA Journal on Uncertainty Quantification*, 1(1):57–78, 2013.
- Poloczek, M., Wang, J., and Frazier, P. I. Warm starting bayesian optimization. In *2016 Winter Simulation Conference (WSC)*, pp. 770–781. IEEE, 2016.
- Poloczek, M., Wang, J., and Frazier, P. Multi-information source optimization. In *Advances in Neural Information Processing Systems*, pp. 4289–4299, 2017.
- Rasmussen, C. E. and Williams, C. K. I. *Gaussian Processes for Machine Learning*. MIT Press, 2004. ISBN 026218253X.
- Sambakhé, D., Rouan, L., Bacro, J.-N., and Gozé, E. Conditional optimization of a noisy function using a kriging metamodel. *Journal of Global Optimization*, 73(3):615–636, 2019.
- Scott, W., Frazier, P., and Powell, W. The correlated knowledge gradient for simulation optimization of continuous parameters using Gaussian process regression. *SIAM Journal on Optimization*, 21(3):996–1026, 2011. ISSN 1052-6234.
- Shahriari, B., Swersky, K., Wang, Z., Adams, R. P., and De Freitas, N. Taking the human out of the loop: A review of bayesian optimization. *Proceedings of the IEEE*, 104(1):148–175, 2015.
- Smith-Miles, K., Baatar, D., Wreford, B., and Lewis, R. Towards objective measures of algorithm performance across instance space. *Computers and Operations Research*, 45:12–24, 2014. ISSN 03050548. doi: 10.1016/j.cor.2013.11.015. URL <http://dx.doi.org/10.1016/j.cor.2013.11.015>.
- Snoek, J., Larochelle, H., and Adams, R. P. Practical bayesian optimization of machine learning algorithms. In *Advances in neural information processing systems*, pp. 2951–2959, 2012.
- Swersky, K., Snoek, J., and Adams, R. P. Multi-task Bayesian optimization. In *Advances in Neural Information Processing Systems*, pp. 2004–2012, 2013.
- Toscano-Palmerin, S. and Frazier, P. I. Bayesian optimization with expensive integrands. *arXiv preprint arXiv:1803.08661*, 2018.
- Wang, Z. and Jegelka, S. Max-value entropy search for efficient bayesian optimization. In *Proceedings of the 34th International Conference on Machine Learning-Volume 70*, pp. 3627–3635. JMLR. org, 2017.
- Wang, Z., Zoghi, M., Hutter, F., Matheson, D., and De Freitas, N. Bayesian optimization in high dimensions via random embeddings. In *Twenty-Third International Joint Conference on Artificial Intelligence*, 2013.
- Xie, J., Frazier, P. I., and Chick, S. E. Bayesian optimization via simulation with pairwise sampling and correlated prior beliefs. *Operations Research*, 64(2):542–559, 2016.

## A. Computing Hybrid Knowledge Gradient

At iteration  $n$  during optimization, let the training inputs be  $\tilde{X}^n = ((s^1, x^1), \dots, (s^n, x^n))$  and the training outputs  $Y^n = (y^1, \dots, y^n)$ . Given a prior mean and kernels functions,  $\mu^0(s, x) : S \times X \rightarrow \mathbb{R}$  and  $k^0(s, x, s', x') : S \times X \times S \times X \rightarrow \mathbb{R}$ . Finally let the new sample point be  $(s, x)^{n+1} = \tilde{x}^{n+1}$ .

### A.1. One-Step Look-ahead Posterior Mean $\mu^{n+1}(s, x)$

Updating the mean function with data from the  $0^{th}$  step to  $n^{th}$  step is given by

$$\mu^n(s, x) = \mu^0(s, x) + \underbrace{k^0(s, x, \tilde{X}^n) K^{-1} (Y^n - \mu^0(\tilde{X}^n))}_{\text{define } \tilde{Y}^n} \quad (10)$$

$$= \mu^0(s, x) + k^0(s, x, \tilde{X}^n) \tilde{Y}^n \quad (11)$$

where  $K = k^0(\tilde{X}^n, \tilde{X}^n)$ .  $\mu^n(s, x)$  may also be written as a weighted average of a modified  $\tilde{Y}^n \in \mathbb{R}^n$  vector as defined above. Computing the new posterior mean reduces to augmenting  $\tilde{X}^n \rightarrow \tilde{X}^{n+1}$  with  $\tilde{x}^{n+1}$  and computing  $\tilde{Y}^{n+1} \in \mathbb{R}^{n+1}$ . A simple change of indices from  $0 \rightarrow n$  and  $n \rightarrow n+1$ , yields the one-step updated posterior mean

$$\mu^{n+1}(s, x) = \mu^n(s, x) + \frac{k^n(s, x, \tilde{x}^{n+1})}{k^n(\tilde{x}^{n+1}, \tilde{x}^{n+1}) + \sigma_\epsilon^2} (y^{n+1} - \mu^n(\tilde{x}^{n+1})). \quad (12)$$

which contains the random  $y^{n+1}$ . This may be factorized as follows:

$$\mu^{n+1}(s, x) = \mu^n(s, x) + k^n(s, x, \tilde{x}^{n+1}) \underbrace{\frac{1}{\sqrt{k^n(\tilde{x}^{n+1}, \tilde{x}^{n+1}) + \sigma_\epsilon^2}}}_{\text{standard deviation of } y^{n+1}} \underbrace{\frac{(y^{n+1} - \mu^n(\tilde{x}^{n+1}))}{\sqrt{k^n(\tilde{x}^{n+1}, \tilde{x}^{n+1}) + \sigma_\epsilon^2}}}_{\text{Z-score of } y^{n+1}} \quad (13)$$

$$= \mu^n(s, x) + k^n(s, x, \tilde{x}^{n+1}) \frac{1}{\sigma_{y^{n+1}}^n(\tilde{x}^{n+1})} Z \quad (14)$$

where the left and centre factors are a deterministic and the right factor is the (at time  $n$ ) stochastic Z-score of the new  $y^{n+1}$  value. This is clear by noting that the predictive distribution of the new output  $y^{n+1}$

$$\mathbb{P}[y^{n+1} | \tilde{x}^{n+1}, \tilde{X}^n, Y^n] = N(\mu^n(\tilde{x}^{n+1}), k^n(\tilde{x}^{n+1}, \tilde{x}^{n+1}) + \sigma_\epsilon^2). \quad (15)$$

as a result, to sample new posterior mean functions, we may simply sample  $Z \sim N(0, 1)$  values and compute Equation 14. However, this results in a quadratic cost per call to sampled poster mean function as both  $k^n(s, x, \tilde{x}^{n+1})$  and  $\sigma_{y^{n+1}}^n(\tilde{x}^{n+1})$  have  $O(n^3)$  quadratic cost. This can be easily reduced to linear instead as we now show.

We next focus on the first factor  $k^n(s, c, \tilde{x}^{n+1})$  which may also be factorized

$$k^n(s, x, \tilde{x}^{n+1}) = k^0(s, x, \tilde{x}^{n+1}) - k^0(s, x, \tilde{X}^n) K^{-1} k^0(\tilde{X}^n, \tilde{x}^{n+1}) \quad (16)$$

$$= \underbrace{[k^0(s, x, \tilde{X}^n), k^0(s, x, \tilde{x}^{n+1})]}_{k^0(s, x, \tilde{X}^{n+1})} \begin{bmatrix} -K^{-1} k^0(\tilde{X}^n, \tilde{x}^{n+1}) \\ 1 \end{bmatrix}. \quad (17)$$

Combining Equations 11 and 17 yields the following formula

$$\mu^{n+1}(s, x) = \mu^0(s, x) + k^0(s, x, \tilde{X}^{n+1}) \left( \begin{bmatrix} \tilde{Y}^n \\ 0 \end{bmatrix} + \frac{Z}{\sigma_{y^{n+1}}^n(\tilde{x}^{n+1})} \begin{bmatrix} -K^{-1} k^0(\tilde{X}^n, \tilde{x}^{n+1}) \\ 1 \end{bmatrix} \right) \quad (18)$$

$$= \mu^0(s, x) + k^0(s, x, \tilde{X}^{n+1}) \tilde{Y}^{n+1}. \quad (19)$$

The quantity  $\tilde{Y}^n$  is pre-computed at the start of the algorithm iteration, the quantity  $-K^{-1} k^0(\tilde{X}^n, \tilde{x}^{n+1})$  has quadratic cost and can be computed once and used again for  $\sigma_{y^{n+1}}^n(\tilde{x}^{n+1})$ . Then, sampling posterior mean functions reduces to sampling  $n_y$  values  $z_1, \dots, z_{n_y} \sim N(0, 1)$  and for each value computing  $\tilde{Y}_1^{n+1}, \dots, \tilde{Y}_{n_y}^{n+1}$ . Then each sampled posterior mean is just the weighted average given by Equation 19.

## A.2. Sampling Posterior Means

To stochastically sample posterior means, one would generate  $Z_{MC} = z_1, \dots, z_{n_y} \sim N(0, 1)$  and use Equation 19. For hybrid Knowledge Gradient we instead use deterministic sampling, let  $\Phi^{-1}(q_i) : [0, 1] \rightarrow \mathbb{R}$  be the inverse cumulative distribution function of the univariate Gaussian, then we set  $Z_{MC} = \{z_1, \dots, z_{n_y}\}$  with values given by

$$z_i = \Phi^{-1}\left(\frac{2i-1}{2n_y}\right)$$

such that the  $z_i$  values are evenly spaced, for example  $n_y = 3$  places values at  $Z_{MC} = \{\Phi^{-1}(1/6), \Phi^{-1}(3/6), \Phi^{-1}(5/6)\}$  or  $n_y = 5$  would yield  $Z_{MC} = \{\Phi^{-1}(1/10), \Phi^{-1}(3/10), \Phi^{-1}(5/10), \Phi^{-1}(7/10), \Phi^{-1}(9/10)\}$ . Always using an odd number of points  $n_y$  ensures there is a point at  $z_i = \Phi(0.5) = 0$  in  $Z_{MC}$  which corresponds to  $\mu^{n+1}(s, x) = \mu^n(s, x)$ . Thus, the discretization includes the policy point  $x = \pi^n(s) = \operatorname{argmax}_x \mu^n(s, x)$ .

## A.3. Finding Optimal Action Discretization for Each State

Since evaluating Equation 19 for many points is a simply matrix multiplication, random search is cheap to evaluate in parallel. After random search, the gradient of Equation 19 with respect to  $(s, x)$  is easily computed, and starting from the best random search point, gradient ascent over  $x \in X$  can be used to find the optimal action. This varies with kernel choice and application, we describe our settings in Section C.3.

We start with a set of sampled means  $\mu_1^{n+1}(s, x), \dots, \mu_{n_z}^{n+1}(s, x)$  and a set of sampled states  $s_1, \dots, s_{n_s}$ . For each state  $s_i$ , the set of  $n_z$  optimal actions  $X_{d,s_i}$  is found by optimizing the  $n_z$  posterior means

$$X_{d,s_i} = \bigcup_{j=1}^{n_z} \left\{ \operatorname{argmax}_x \mu_j^{n+1}(s_i, x) \right\}$$

Finally, for each point in the  $\{s_i\} \times X_{d,s_i} = \tilde{X}_{d,s_i}$  (state, action) discretization, we evaluate two quantities, firstly the vector of current posterior means  $\underline{\mu}_{s_i} \in \mathbb{R}^{n_z}$ ,

$$\underline{\mu}_{s_i} = \mu^n(\tilde{X}_{d,s_i}) \tag{20}$$

$$= \mu^0(\tilde{X}_{d,s_i}) + k^0(\tilde{X}_{d,s_i}, \tilde{X}^n) \tilde{Y}^n \tag{21}$$

and the vector of additive updates  $\underline{\sigma}_{s_i} \in \mathbb{R}^{n_z}$ ,

$$\underline{\sigma}_{s_i} = \frac{k^n(\tilde{X}_{d,s_i}, \tilde{x}^{n+1})}{\sigma_{y^{n+1}}^n(\tilde{x}^{n+1})} \tag{22}$$

$$= k^0(\tilde{X}_{d,s_i}, \tilde{X}^{n+1}) \begin{bmatrix} -K^{-1}k^0(\tilde{X}^n, \tilde{x}^{n+1}) \\ 1 \end{bmatrix} \frac{1}{\sigma_{y^{n+1}}^n(\tilde{x}^{n+1})}. \tag{23}$$

These two vectors  $\underline{\mu}_{s_i}$  and  $\underline{\sigma}_{s_i}$  are both differentiable  $\nabla_{\tilde{x}^{n+1}} \underline{\mu}_{s_i}$  and  $\nabla_{\tilde{x}^{n+1}} \underline{\sigma}_{s_i}$  and they are used to analytically compute the peicewise-linear  $\mathbb{E}_Z \left[ \max \left( \underline{\mu}_{s_i} + Z \underline{\sigma}_{s_i} \right) \right] - \max \underline{\mu}_{s_i}$  which is also differentiable. Thus assuming fixed  $\tilde{X}_{d,s_1}, \dots, \tilde{X}_{d,s_{n_s}}$ , approximate gradients are computed and can be used in any stochastic gradient ascent optimizer.

## A.4. Evaluating Knowledge Gradient by Discretization

This algorithm was originally proposed by (Frazier et al., 2009) and we duplicate it here for completeness.

## B. Entropy Based Methods for Conditional Bayesian Optimization

Given a GP model and a dataset,  $\mathbb{P}[x^* | \tilde{X}^n, Y^n]$  is the distribution over the peak of realizations of GP sample functions (abusing notation)  $\mathbb{P}[x^* | \tilde{X}^n, Y^n] = \operatorname{argmax}_x GP(\mu^n(x), k^n(x, x'))$ . Given a new sample input  $x^{n+1}$ , the outcome  $\mathbb{P}[y^{n+1} | x^{n+1}, \tilde{X}^n, Y^n]$  is also a random variable that is Gaussian. For this section, to reduce cluttering notation, we suppress

**Algorithm 1** This algorithm takes as input a set of linear functions parameterised by a vector of intercepts  $\underline{\mu}$  and a vector of gradients  $\underline{\sigma}$ . It then computes the intersections of the piece-wise linear epigraph (ceiling) of the functions and the expectation of the output of the function given Gaussian input. Vector indices are assumed to start from 0.

**Require:**  $\underline{\mu}, \underline{\sigma} \in \mathbb{R}^{n_A}$

```

 $\alpha \leftarrow \operatorname{argmax} \underline{\mu}$ 
 $O \leftarrow \operatorname{order}(\underline{\sigma})$  # get sorting indices of increasing  $\underline{\sigma}$ 
 $\underline{\mu} \leftarrow \underline{\mu}[O], \underline{\sigma} \leftarrow \underline{\sigma}[O]$  # arrange elements
 $I \leftarrow [0, 1]$  # indices of elements in the epigraph
 $\tilde{Z} \leftarrow [-\infty, \frac{\mu_0 - \mu_1}{\sigma_1 - \sigma_0}]$  # z-scores of intersections on the epigraph
for  $i = 2$  to  $n_z - 1$  do
     $\text{endloop} \leftarrow \text{False}$ 
    repeat
         $j \leftarrow \text{last}(I)$ 
         $z \leftarrow \frac{\mu_i - \mu_j}{\sigma_j - \sigma_i}$ 
        if  $z < \text{last}(\tilde{Z})$  then
            Delete last element of  $I$  and of  $\tilde{Z}$ 
        else
            Add  $i$  to end of  $I$  and  $z$  to  $\tilde{Z}$ 
             $\text{endloop} \leftarrow \text{True}$ 
        end if
    until  $\text{endloop}$ 
end for
 $\tilde{Z} \leftarrow [\tilde{Z}, \infty]$ 
 $\underline{A} \leftarrow \phi(\tilde{Z}[1 :]) - \phi(\tilde{Z}[: -1])$  # assuming python indexing
 $\underline{B} \leftarrow \Phi(\tilde{Z}[1 :]) - \Phi(\tilde{Z}[: -1])$ 
 $\text{KG} \leftarrow \underline{B}^T \underline{\mu}[I] - \underline{A}^T \underline{\sigma}[I] - \max \underline{\mu}$  # compute expectation
 $\nabla_{\underline{\mu}} \text{KG}, \nabla_{\underline{\sigma}} \text{KG} \leftarrow \underline{0}$  # initialize gradient vectors with zeros
 $\nabla_{\underline{\mu}} \text{KG}[\alpha] \leftarrow -1$ 
 $\nabla_{\underline{\mu}} \text{KG}[O][I] \leftarrow \underline{B}$  # (numpy indexing) assign to sorted elements on the epigraph
 $\nabla_{\underline{\sigma}} \text{KG}[O][I] \leftarrow -\underline{A}$  # assign to sorted elements on the epigraph
return  $\text{KG}, \nabla_{\underline{\mu}} \text{KG}, \nabla_{\underline{\sigma}} \text{KG}$ 

```

the dependence on  $\tilde{X}^n, Y^n$ . The mutual information between random variables  $y^{n+1}$  and  $x^*$  is defined as

$$\text{MI}(x) = \int_{x^*} \int_{y^{n+1}} \log \left( \frac{\mathbb{P}[y^{n+1}, x^*]}{\mathbb{P}[y^{n+1}] \mathbb{P}[x^*]} \right) \mathbb{P}[y^{n+1}, x^*] dy^{n+1} dx^* \quad (24)$$

where  $\mathbb{P}[y^{n+1}]$  depends upon  $x^{n+1}$  yet we drop it for convenience.

### B.1. Entropy Search

The Entropy search algorithm decomposes the above expression using  $\mathbb{P}[y^{n+1}, x^*] = \mathbb{P}[y^{n+1}] \mathbb{P}[x^* | y^{n+1}]$  resulting in the following acquisition function

$$\text{ES}(x) = \int_{x^*} \log(\mathbb{P}[x^*]) \mathbb{P}[x^*] dx^* + \int_{y^{n+1}} \int_{x^*} \log(\mathbb{P}[x^* | y^{n+1}]) \mathbb{P}[x^* | y^{n+1}] dx^* \mathbb{P}[y^{n+1}] dy^{n+1} \quad (25)$$

$$= H[x^*] - \int_{y^{n+1}} H[x^* | y^{n+1}] \mathbb{P}[y^{n+1}] dy^{n+1} \quad (26)$$

where  $H[x^*]$  is the entropy of the distribution  $\mathbb{P}[x^*]$ . For the conditional case, the outcome  $\mathbb{P}[y^{n+1} | (s, x)^{n+1}]$  is still a Gaussian random variable, and we measure the mutual information with the peak  $x_{s_i}^*$  over actions constrained to a given state  $\{s_i\} \times X$  that is  $\mathbb{P}[x_{s_i}^*] = \operatorname{argmax}_x GP(\mu^n(s_i, x), k^n(s_i, x, s_i, x'))$ . And the conditional entropy search acquisition

function is simply

$$\text{ES}_c(s_i; (s, x)^{n+1}) = H[x_{s_i}^*] - \int_{y^{n+1}} H[x_{s_i}^* | y^{n+1}] \mathbb{P}[y^{n+1}] dy^{n+1}. \quad (27)$$

## B.2. Predictive Entropy Search

We again drop the dependence on  $x^{n+1}$  in  $\mathbb{P}[y^{n+1} | x^{n+1}]$ . The Predictive Entropy search algorithm uses an alternative decomposition of the Mutual Information using  $\mathbb{P}[y^{n+1}, x^*] = \mathbb{P}[y^{n+1} | x^*] \mathbb{P}[x^*]$  resulting in the following acquisition function

$$\text{PES}(x) = H[y^{n+1}] - \int_{x^*} H[y^{n+1} | x^*] \mathbb{P}[x^*] dx^*. \quad (28)$$

For the conditional case, the outcome  $\mathbb{P}[y^{n+1} | (s, x)^{n+1}]$  is still a Gaussian random variable, and we measure the mutual information with the peak  $x^*$  constrained to a given state  $s_i$  that is as above  $\mathbb{P}[x_{s_i}^*] = \text{argmax}_x GP(\mu^n(s_i, x), k^n(s_i, x, s_i, x'))$ . And the conditional predictive entropy search acquisition function is simply

$$\text{PES}_c(s_i; (s, x)^{n+1}) = H[y^{n+1}] - \int_{x_{s_i}^*} H[y^{n+1} | x_{s_i}^*] \mathbb{P}[x_{s_i}^*] dx^* \quad (29)$$

where the expression  $H[y^{n+1} | x_{s_i}^*]$  is the (non Gaussian) distribution of  $y^{n+1}$  at  $(s, x)^{n+1}$  given that the peak of state  $s_i$  is at  $x_{s_i}^*$ .

## B.3. Max Value Entropy Search

Max value entropy search instead measures the mutual information between the new outcome  $\mathbb{P}[y^{n+1} | x^{n+1}]$  and the largest possible outcome (again abusing notation)  $\mathbb{P}[y^*] = \max_x GP(\mu^n(x), k^n(x, x'))$ , the peak value of posterior sample functions. The acquisition function decomposes the mutual information into

$$\text{MES}(x) = H[y^{n+1}] - \int_{y^*} H[y^{n+1} | y^*] dy^* \quad (30)$$

The conditional version measures the mutual information between  $\mathbb{P}[y^{n+1} | (s, x)^{n+1}]$  and the largest  $y$  value amongst all outcomes with the same state  $\mathbb{P}[y_{s_i}^*] = \max_x GP(\mu^n(s_i, x), k^n(s_i, x, s_i, x'))$

$$\text{MES}(s_i, (s, x)^{n+1}) = H[y^{n+1}] - \int_{y_{s_i}^*} H[y^{n+1} | y_{s_i}^*] \mathbb{P}[y_{s_i}^*] dy_{s_i}^* \quad (31)$$

## C. Implementation Details

### C.1. REVI

At iteration  $n$  of the algorithm, we used a discretization of size  $n_{disc} = 2n$ , split equally amongst actions and states  $n_s = n_x = \lceil \sqrt{n_{disc}} \rceil$ . States are sampled from  $\mathbb{P}[s]$  and actions are sampled as a latin hypercube over  $X$ . The acquisition function is optimized by 100 points of random search over  $S \times X$  followed by Nelder-Mead ascent starting from the best 20 points in the random search phase.

### C.2. MTS

We use a target discretization size of  $n_{disc} = 3000$ . Given  $d_s$  states dimensions and  $d_x$  action dimensions, we sampled states uniformly, the number of sampled states is given by  $n_s = \lceil (n_{disc})^{d_s / (d_s + d_x)} \rceil$  and the number of actions per state is  $n_x = \lceil n_{disc} / n_s \rceil$  such that  $n_s * n_x \approx n_{disc}$ . This way the discretization over all states and action dimensions is roughly constant. For each sampled state  $s_i$ ,  $n_x$  actions are generated in three ways. Firstly, the policy is evaluated  $x_{s_i}^\pi = \pi^n(s_i)$ , we generate 40 actions around this policy action. Secondly, we take the 10 nearest neighbor states from the training set, and the points with the 4 largest  $y$  values are added to the discretization set with randomly generated neighbors. Finally, remaining actions in the  $n_x$  budget come from uniform random sampling over  $X$ . Each  $s_i$  has a bespoke action discretization. Sampled functions are drawn using the python numpy random normal generate function.

### C.3. ConBO

Each sampled posterior mean function was optimized in two steps. For a given state  $s_i$ , firstly, the action discretization used by MTS, reduced to 40 points in total was used in parallel random search. The best point was then used in conjugate-gradient ascent for 20 steps.

For optimizing sampled posterior mean functions for which  $z_i = 0$ , that is  $\mu^{n+1}(s, x) = \mu^n(s, x)$ , this given by the policy  $x_{s_i}^\pi = \pi^n(s_i)$ . Since the same, or very similar states, may be used multiple times for different ConBO( $(s, x)^{n+1}$ ) calls, we may use caching to avoid such repeated policy computation. Whenever the policy is queried for the optimal action for a given state, the final (state, action) pair are stored in a lookup table. Any future calls to the policy function with state  $s_j$  can check the lookup table and if very similar states exists use the same action, if a somewhat similar state exists, re-optimize the action, if no similar states exist perform a full optimization as above.

In our experiments, the cache of stored policy calls is wiped clean before any testing, ConBO is not given an unfair advantage at test time. In practical applications, this need not be the case.

## D. Further Experiments

We run a range of alternative methods on all benchmarks in serial mode. We then repeat the serial and batch mode experiments from the main paper with the squared exponential (SE) kernel instead of Matérn.

### D.1. Alternative Baselines

- **KNN:** we collect data randomly with states from the state distribution and actions uniformly at random. The policy takes a state, finds the  $k = 10$  nearest neighbors in Euclidean distance, and returns the action with the largest observed output. This is a model-free, non-Bayesian, non-learning method and serves as the simplest worst case algorithm.
- **UNI:** Data is randomly collected as with KNN. However, a GP with Matérn kernel is fit and the policy takes a state and returns the best predicted action.
- **EI:** Standard global optimization expected improvement. We fit a GP with Matérn kernel as with all BO methods. Data acquisition is according to expected improvement, treating the state variables as dimensions to be optimized. The policy takes a state and returns the best predicted action.

Figure 7 shows results with the alternative baselines on the synthetic benchmarks. On this ideal low-dimensional setting, ConBO is significantly the strongest algorithm.

Figure 8 shows results with the alternative baselines on the Assemble to Order and Ambulances benchmarks. In this more difficult setting where model fitting is more of a concern, we see EI performs well and is the best algorithm for small budgets while model fit is still very poor. For larger budgets ConBO catches up and surpasses in the case of ATO.

### D.2. Squared Exponential Kernel

To investigate the effect of changing the kernel, we also ran the more difficult benchmarks with the squared exponential kernel. The ATO problem sees an overall decrease in performance across all methods suggesting this benchmark is sensitive to model misspecification. The Ambulances problem sees no change in performance, Matérn and squared exponential kernels both work well. See Figure 9.

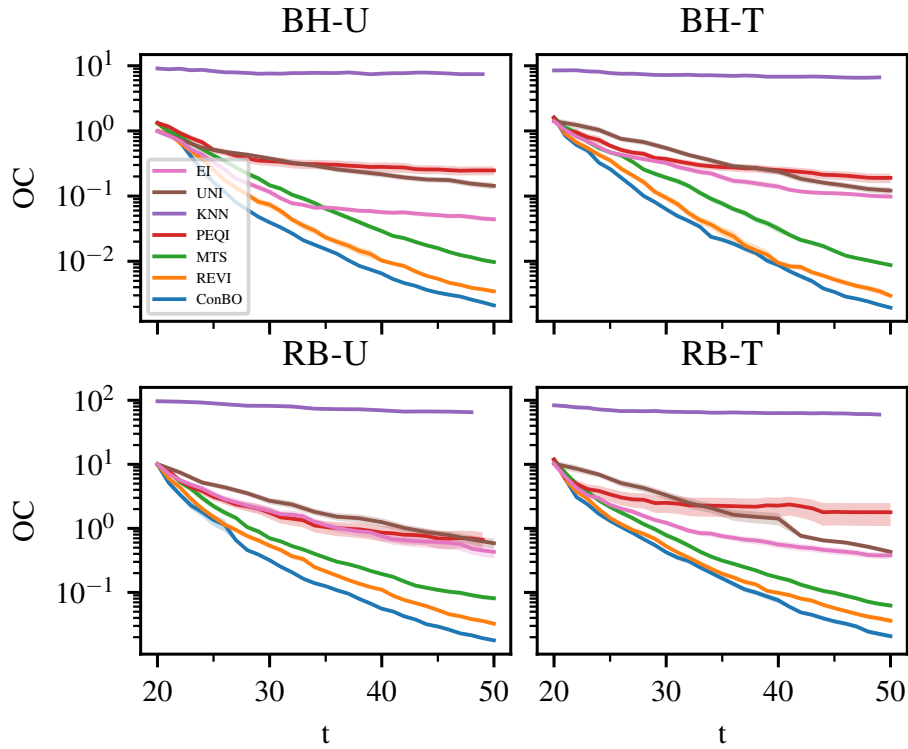


Figure 7. Test function opportunity cost. Top row: Branin-Hoo function with uniform (U) and triangular (T) state distributions. Bottom row: Rosenbrock function. The experiments were averaged over 100 trials and show the mean value and standard error. Surprisingly, EI performs very well for small budgets. On ATO only ConBO outperforms EI for larger budget. On Ambulances, the difference between ConBO and EI are not statistically significant.

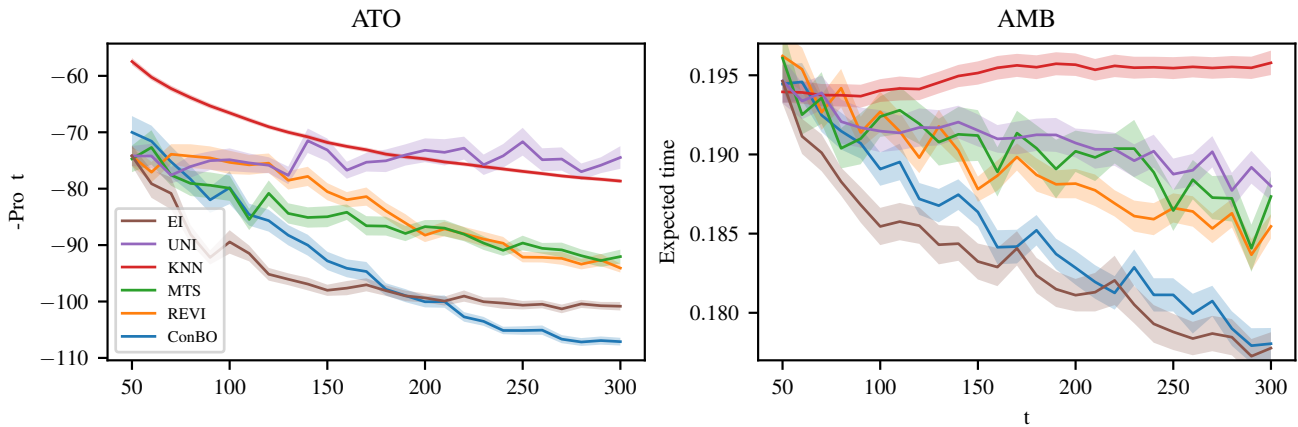


Figure 8. Algorithm performance on the Assemble To Order (left) and Ambulances (right) benchmarks with Matérn kernel. The experiments were averaged over 100 trials and show the mean value and standard error.



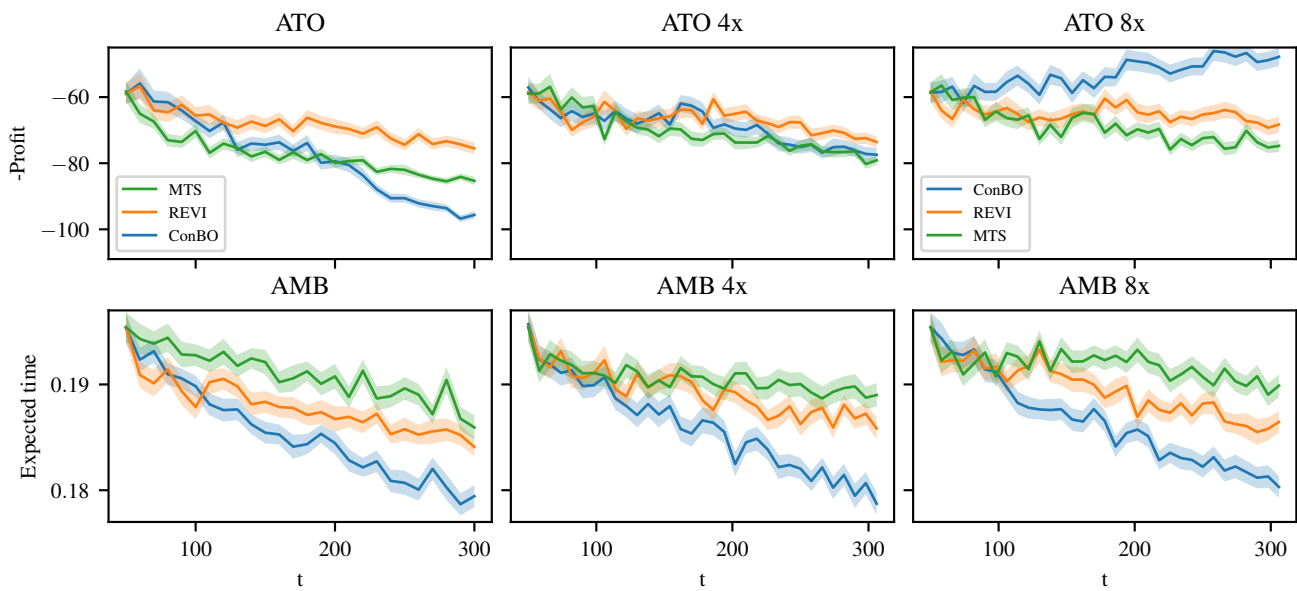


Figure 9. Algorithm performance on the Assemble To Order (top) and Ambulances (bottom) benchmarks with squared exponential kernel. The left-most plots are with serial sample collection whilst 4x and 8x denote results with parallel sample collection with batch sizes of 4 and 8 points respectively. The experiments were averaged over 100 trials and show the mean value and standard error.